

Effect of Microwave Frequency on Hydrothermal Synthesis of Nanocrystalline Tetragonal Barium Titanate

Edward K. Nyutu,[§] Chun-Hu Chen,[§] Prabir K. Dutta,[‡] and Steven L. Suib^{*,§,†}

Department of Chemistry and Department of Chemical, Materials and Bimolecular Engineering, University of Connecticut, Storrs, Connecticut 06269 and Department of Chemistry, The Ohio State University, Columbus, Ohio 43210

Received: November 28, 2007; Revised Manuscript Received: April 29, 2008

Nanocrystalline tetragonal barium titanate (BaTiO_3) with particle sizes ranging from 30 to 100 nm were synthesized via microwave-hydrothermal routes at various fixed microwave frequencies and also using variable frequency with 1–5 s sweep times. The effects of microwave frequency, microwave bandwidth sweep time, and aging time on the microstructure, particle sizes, phase purity, surface areas, and porosities of the as-prepared BaTiO_3 were investigated systematically. The crystallized BaTiO_3 powders were characterized by X-ray diffraction, Raman spectroscopy, thermal analysis, infrared spectroscopy, field emission scanning electron microscopy, and transmission electron microscopy with an EDS analyzer. The results show that the particle sizes, morphologies, and surface areas of the products are influenced by the microwave frequency and bandwidth sweep time. High microwave frequency (5.5 GHz) and variable frequency (3–5.5 GHz to 1 s) led to spherical particles with narrow and more uniform particle size distributions. BaTiO_3 prepared using the standard 2.45 GHz yielded particles with a cubic microstructure. The surface areas of the prepared powders decreased with aging time using 4.0 and 5.5 GHz, but increased gradually with extended aging time in variable frequency (3–5.5 GHz to 1 s) processing. The dependence of properties of barium titanate on microwave frequency could be due to different transverse magnetic modes at different frequencies. For comparison purposes, conventional hydrothermal experiments were also performed under similar conditions as in microwave hydrothermal routes.

Introduction

Barium titanate (BaTiO_3), with a perovskite-type structure is a technologically important material because of its ferroelectric response and high dielectric constant.^{1,2} BaTiO_3 has a wide range of applications in electronic and electro-optic devices, such as thermistors, multilayer ceramic capacitors, microwave absorbers, and transducers.¹ Transition metal oxides with reduced dimensions may possess unique properties that are size-dependent and cannot be determined by extrapolation of bulk characteristics.³ For instance, the displacive transformation in BaTiO_3 nanomaterials is suppressed and the cubic phase was found to be stable at room temperature.¹ Recent progress in electronic technologies requires finer BaTiO_3 particles with particles sizes of up to 100 nm in order to make progressive multilayer ceramic condensers with a high density and capacity.⁴ Recently, there has been tremendous interest in the development of methods to fabricate barium titanate with different morphologies, particle sizes, and dispersions.

Barium titanate exists in several polymorphic forms, of which the tetragonal (ferroelectric) and cubic (paraelectric) phases have been investigated extensively.^{1,2} The properties of BaTiO_3 are usually dependent on the particle size, purity, dispersability, and homogeneity of the prepared powder.¹ These properties are affected mainly by the sample preparation procedures.^{1–3} Several methods have been employed to prepare barium titanates with

TABLE 1: Summary of the Experimental Conditions and Results^a

sample	microwave frequency (GHz)	time (h)	phases detected by XRD	phases detected by Raman
1	2.45	2	C, BC	Td
2	4.00	2	C, BC	Td
3	5.50	2	C	Td
4	3–5.5, sweep 1 s	2	C	Td
5	2.45	10	C	Td
6	4.00	10	C, BC	Td
7	5.50	10	C	Td
8	3–5.5, sweep 1 s	10	C	Td
9	2.45	20	C	Td
10	4.00	20	C, BC	Td, Hex
11	5.50	20	C	Td
12	3–5.5, sweep 1 s	20	C	Td
13	3–5.5, sweep 5 s	20	C, BC	Td, Hex
14	CH	20	C	Td
15	5.50	40	C, BC	Td, Hex
16	3–5.5, sweep 1 s	40	C, BC	Td
17	CH	40	C, BC	Td

^a C, cubic- BaTiO_3 ($Pm\bar{3}m$ symmetry); Td, tetragonal BaTiO_3 ($P4mm$ symmetry); Hex, hexagonal BaTiO_3 ($P6_3mmc$ symmetry); BC, trace barium carbonate. All experiments were performed at 170 °C and total volume, 40 cm³ in a sealed autoclave of the same size and volume.

various particle sizes and morphologies. Hydrothermal techniques that include conventional, microwave-assisted, and solvothermal routes have been found to be successful for the synthesis of ultrafine (nano-/microsize) barium titanate powders.^{1–3,5–9} The conventional hydrothermal (CH) method is a

* Corresponding author. Phone: (860) 486-2797. Fax: (860) 486-2981. E-mail: steven.suib@uconn.edu.

[§] Department of Chemistry, University of Connecticut.

[†] Department of Chemical, Materials, and Bimolecular Engineering, University of Connecticut.

[‡] The Ohio State University.

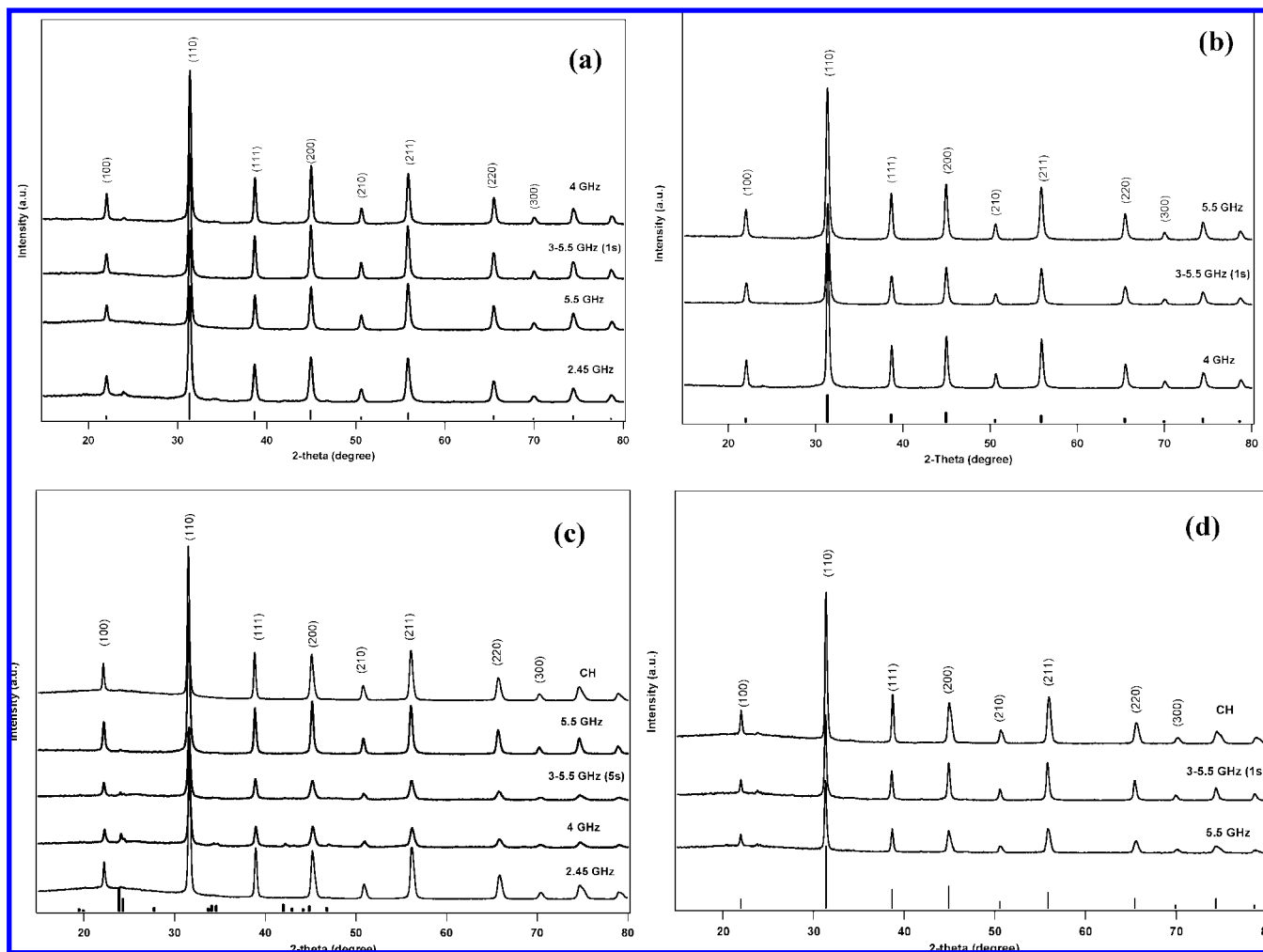


Figure 1. X-ray powder diffraction patterns of barium titanate prepared for (a) 2, (b) 10, (c) 20, and (d) 40 h by MH at various microwave frequencies or CH processes at 170 °C. XRD patterns collected from the CH (2 and 10 h) samples are almost identical to patterns (a) 4 GHz and (b) 5.5 GHz, respectively. Vertical solid lines below the patterns a, b, and d correspond to the positions of the Bragg reflections for cubic barium titanate (JCPDS no. 31-174). Patterns below c correspond to the byproduct orthorhombic BaCO₃ (JCPDS no. 5-378).

time-consuming process that takes several hours to days.⁶ The microwave hydrothermal (MH) process has been found to reduce both the synthesis times and temperatures.^{2,9,10} Microwave heating has reduced the synthesis time and enhanced the processing of BaTiO₃; however, studies on the effects of microwave synthesis at different frequencies are lacking. For all microwave hydrothermal syntheses of BaTiO₃, the primary frequency utilized has been the standard 2.45 GHz.

Microwave heating is affected by mainly two factors; permittivity (dielectric constant) (ϵ'), which is the extent to which the electric field is able to produce a polarized response in a molecule or assembly of molecules, and dielectric loss (ϵ''), which is indicative of the ability of a medium to convert dielectric energy to heat.^{11,12} The dependence of the heating rate is given by ϵ''/ϵ' , defined as loss tangent ($\tan \delta$). Dielectric loss tangent ($\tan \delta$) depends on the temperature, composition, and physical state of the reactants and the frequency of the electromagnetic waves.¹²

Recent work by our group shows that microwave frequency plays an important role in the catalytic oligomerization of methane and in the catalytic activity and morphologies of manganese oxide octahedral molecular sieves.^{13–15} Caponetti and co-workers also showed the effect of microwave frequency (2.45–18 GHz) on particle size distribution of prepared CdS. They observed that larger particles were produced at 12 GHz,

as compared to those produced at 2.45, 2.85, 8, and 18 GHz and those produced by conventional heating.¹⁶ Since different vessel sizes were used in this work, recent findings by Conner and co-workers suggest that the surface-to-volume ratio of the irradiated solution and the reactor geometry are also important, and therefore, in this case, these effects must be considered.^{11,17} Recently, barium titanate has been studied as a microwave-absorbing material with potential to eliminate unwanted electromagnetic signals that cause electromagnetic interference problems.¹⁸

In this work, we systematically investigated the effects of microwave frequency, bandwidth sweep time, and processing time on the particle size, phase, microstructure, and porosity of barium titanate prepared by microwave hydrothermal and compared them with results obtained with conventional hydrothermal processes. In variable frequency, the sweep time is the specified time during which the selected bandwidth is swept around the central frequency.¹³ Several microwave frequencies were explored: fixed frequencies of 2.45, 4.0, and 5.5 GHz and a variable frequency of 3–5.5 GHz, bandwidth frequency of 1.25 GHz, and 1–5 s sweep times. The reaction mixture and the reactor size in all the experiments was the same, and the temperature was maintained at 170 °C for 2–40 h.

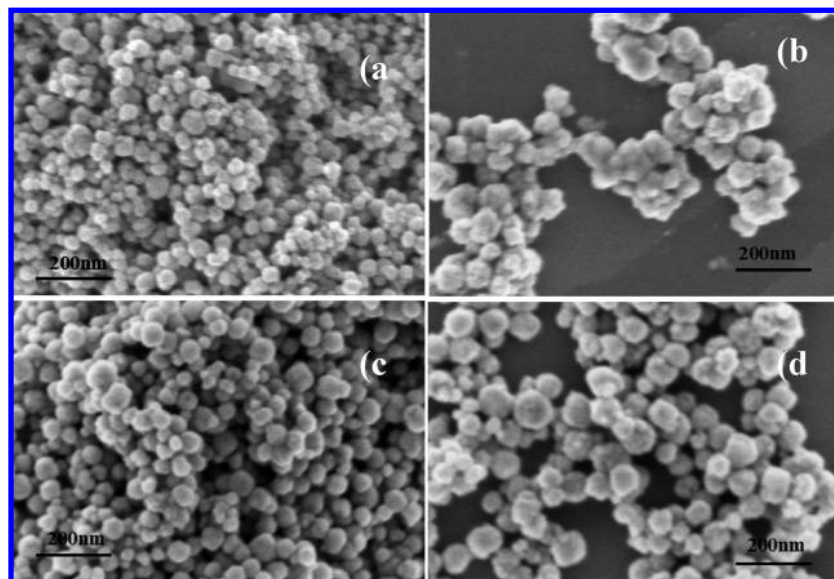


Figure 2. FESEM images of samples prepared at different microwave frequencies for 2 h: (a) 2.45 GHz; (b) 4.0 GHz; (c) 5.5 GHz; and (d) 3–5.5 GHz, 1 s sweep time.

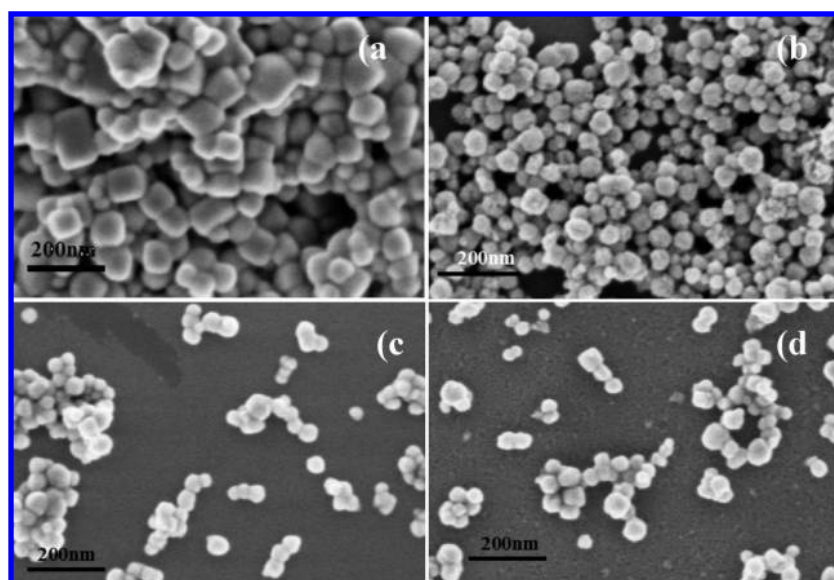


Figure 3. FESEM images of samples prepared at different microwave frequencies for 10 h: (a) 2.45 GHz; (b) 3–5.5 GHz (1 s); (c) 4.0 GHz; and (d) 5.5 GHz, 1 s sweep time.

Experimental Methods

Starting Materials. BaCl₂·2H₂O (J. T. Baker, 98%), NaOH (J. T. Baker), titanium (IV) isopropoxide (Aldrich, 98%), and HCl (J. T. Baker, 33–40%).

Microwave/ Conventional Hydrothermal Synthesis. The synthesis solution was prepared as reported by Ma et al.² Briefly, 20 mmol of barium chloride dehydrate was dissolved in a suspension of 12 mmol of hydrated titanium dioxide prepared by the hydrolysis of titanium (IV) isopropoxide with 1 M HCl followed by washing and centrifugation. About 15 min later, 20 mmol of sodium hydroxide pellets were added to the mixture. The mixture was purged with nitrogen to prevent the formation of barium carbonate. The mixture (40 cm³) was then transferred to a PTFE (CEM Corp., Matthews, NC) autoclave, sealed, and placed in the microwave chamber. Models LT-502 Xb and MMT 10–1300 microwave reactor systems were used for the study. Both furnaces have a temperature and power control program, and a shielded thermocouple was directly inserted into

the reaction mixture for temperature measurements. The vessel was kept at 170 °C for 2–40 h under fixed or variable microwave frequencies ranging from 2.45 to 5.5 GHz for a fixed frequency or 3–5.5 GHz in a variable frequency (VFMW) range with a sweeping time of 1–5 s. The microwave power was generated at ~200–300 W during the synthesis. For 20 h microwave aging, at least two experiments were carried out for each frequency studied. For comparison, CH experiments were also performed in a PTFE vessel (100 cm³) placed inside a stainless steel autoclave. The volume and concentration of the precursors were maintained as in the MH process. The autoclave was sealed and kept at 170 °C for 2–40 h under autogenous pressure. The products of the MH process and those of the CH process were centrifuged, washed several times with distilled water, and then dried overnight at 80 °C.

Characterization. The products were analyzed by X-ray diffraction (XRD) to determine their purity and crystallinity using a Scintag X-ray diffractometer with Cu K_α X-ray radiation

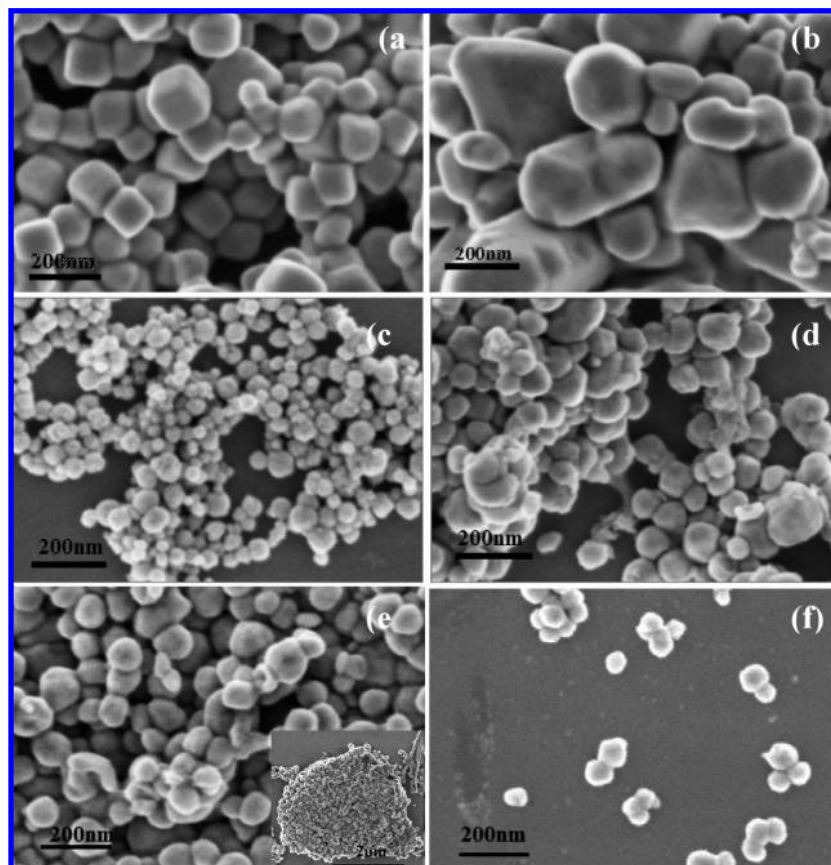


Figure 4. FESEM images of samples prepared at different microwave frequencies for 20 h: (a) 2.45 GHz; (b) CH GHz; (c) 5.5 GHz; (d) 4.0 GHz; (e) 3–5.5 GHz (5 s); and (f) 3–5.5 GHz, 1 s sweep time.

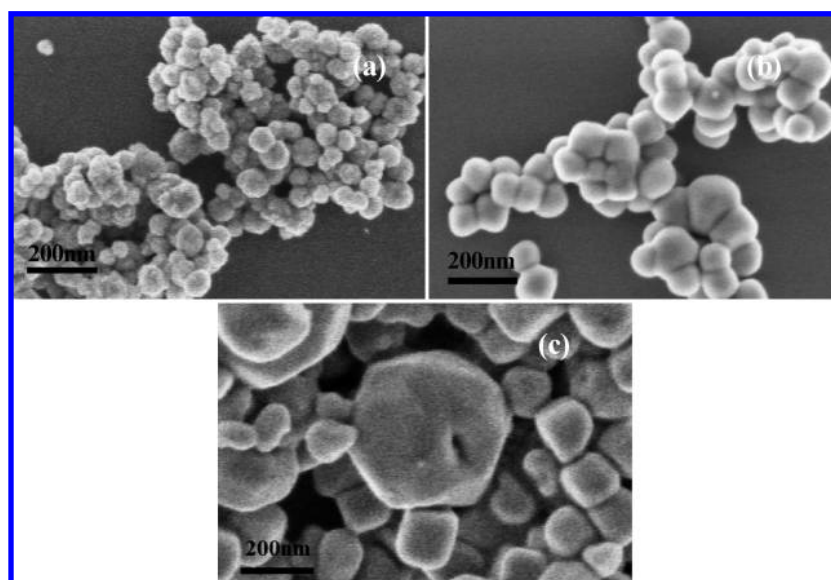


Figure 5. FESEM images of samples prepared at different conditions for 40 h: (a) using variable frequencies (3–5.5 GHz, 1 s), (b) fixed frequency (5.5 GHz), and (c) conventional heating.

with a 1.5418 Å wavelength. A beam voltage of 45 kV and a 40 mA beam current were used. Phases present were identified using a JCPDS database. The size of the barium titanate crystallites was calculated by means of the Scherrer equation from the line-broadening of the (100), (110), and (111) reflections. The instrumental line-broadening was corrected using a LaB₆ standard. The size and morphology of the product particle were studied using field emission scanning electron microscopy (FESEM) on a Zeiss DSM 982 Gemini instrument

with a Schottky emitter at an accelerating voltage of 2 kV and a beam current of 1 μA. The samples were suspended in ethanol and dispersed on AuPd-coated silicon chips previously mounted onto a stainless steel sample holder using a two-sided carbon tape.

The products were further characterized by transmission electron microscopy (TEM) with a JEOL 2010 FastEM at an accelerating voltage of 200 kV with an EDS analyzer. The samples were prepared by dispersing the materials in ethanol.

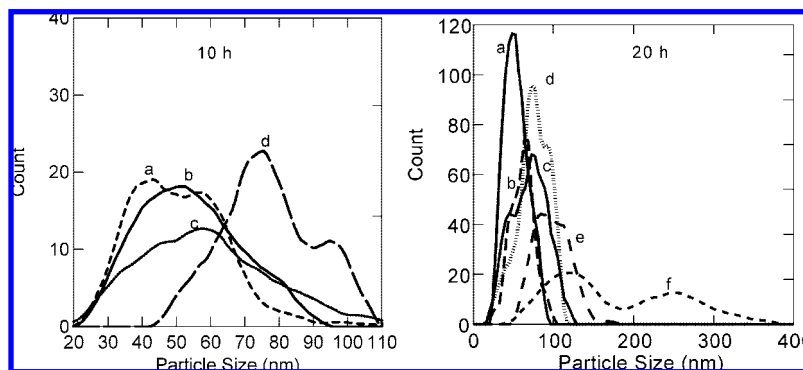


Figure 6. Particle size distributions of BaTiO₃ prepared under different microwave frequencies at 170 °C for 10 h: (a) 3–5.5 GHz, 1 s; (b) 5.5 GHz; (c) 4 GHz; and (d) 2.45 GHz. For 20 h: (a) 5.5 GHz; (b) 3–5.5 GHz, 1 s; (c) 3–5.5 GHz, 5 s; (d) 4 GHz; (e) 2.45 GHz; and (f) CH.

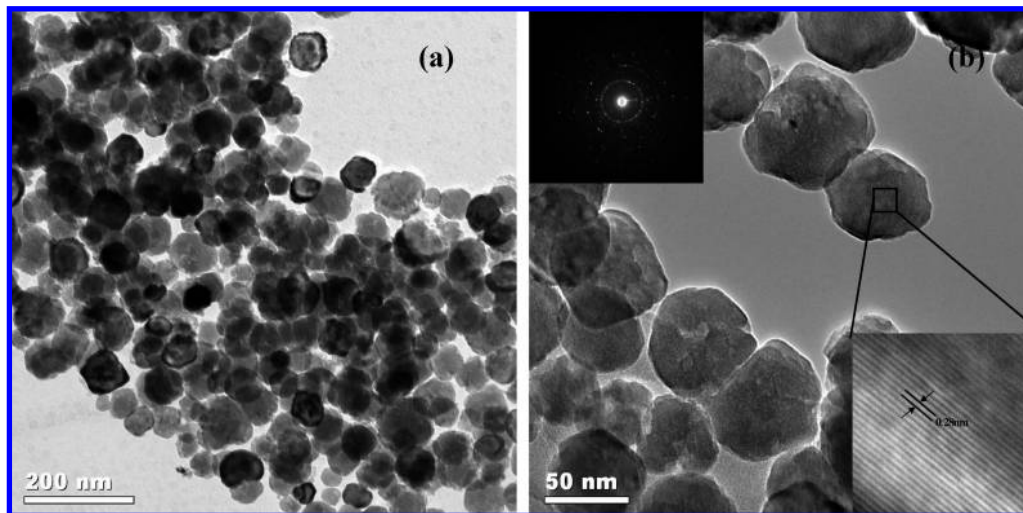


Figure 7. TEM images of BaTiO₃ prepared at 3–5.5 GHz (1s) for 20 h at 170 °C: (a, b) low magnification, top insert in (b) show the corresponding SAED patterns, insert (bottom) shows a high magnification of (b).

A drop of the dispersion was then placed onto a carbon-coated Cu grid and allowed to dry. Particle size distributions were obtained by processing of the FESEM images with ImageJ software.¹⁹ About 100–200 particles were counted in SEM micrographs. Thermogravimetric analysis (TGA) techniques were employed to study the thermal stability of the samples. The experiments were performed with a TA instrument model 2950 in a N₂ atmosphere. The temperature was increased from 30 to 900 °C at a rate of 10 °C/min during the experiments. Room temperature Raman measurements were obtained on a Renishaw 2000 Ramascope with a 514.5 nm Ar⁺ laser as the excitation source. Prior to each measurement, the spectrometer was calibrated using a silicon wafer. Raman scattering was utilized to identify the phase composition of the particles. Fourier transform infrared (FT-IR) spectra were recorded on a Nicolet Magna-IR system 750 spectrometer at room temperature. Total surface area was calculated from the N₂ adsorption isotherms on a Micromeritics ASAP 2010 surface analyzer according to the BET (Brunauer–Emmett–Teller) method. Duplicate experiments were performed for each sample.

Results

The effects of microwave frequency, sweep time (1–5 s), and irradiation time (2–40 h) on the particle size, phase composition, and microstructures of barium titanate prepared by microwave hydrothermal and conventional hydrothermal processes were investigated. A summary of the experimental conditions and results is shown in Table 1.

X-ray Diffraction. The XRD patterns of the samples prepared for 2–40 h using different microwave frequencies via the MH and those prepared with the CH process are shown in Figure 1 a–d. All the reflections can be indexed as being barium titanate with a perovskite-type cubic structure (Joint Committee on Powder Diffraction Standards (JCPDS) card no. 31-174). Barium titanate was obtained after 2 h, but previous studies suggest longer aging time is required to ensure complete crystallization.^{2,9,10} The crystal symmetry of the prepared nanoparticles could not be determined with certainty to be either tetragonal or cubic from the XRD patterns. There was no apparent splitting of the (002)/(200), (201)/(210), and (112)/(211) peaks in the 2θ = 40–56° region for the samples prepared for 2–40 h by either MH or CH. However, the (111) peak of samples obtained after 20 and 40 h is appreciably narrower than that of the (200) peak, an indication of the existence of a polar and probably tetragonal structure. No other impurity peaks were detected by XRD except for orthorhombic BaCO₃ (JCPDS no. 5-378), as illustrated in Figure 1b.

Field Emission Scanning Electron Spectroscopy. The microstructures of barium titanate prepared under various conditions are shown in Figures 2–5. The corresponding representative particle size distributions of barium titanate particles obtained under various microwave frequencies, aging times, and in a conventional hydrothermal process are shown in Figure 6. The BaTiO₃ particles obtained after 2 h of microwave hydrothermal aging using 2.45 and 5.5 GHz were fairly uniform and had an average diameter of 47 ± 11 and 55

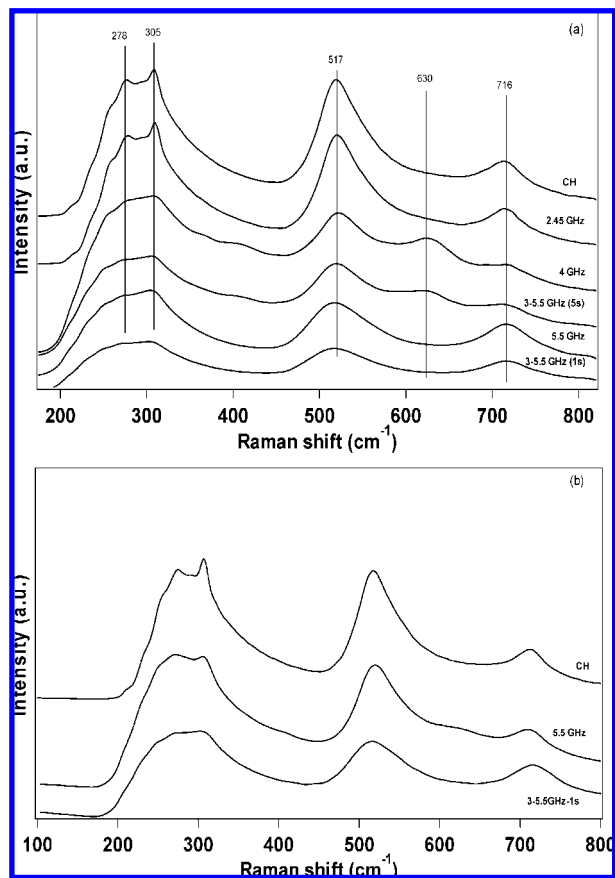


Figure 8. Raman spectra of BaTiO₃ prepared by MH at various microwave frequencies and by CH for (a) 20 and (b) 40 h.

± 13 nm, respectively (Figure 2a, c). Usage of 4.0 GHz and variable frequencies (3–5.5 GHz to 1 s) resulted in larger and less uniform products with an average diameter of 77 ± 15 and 67 ± 18 nm, respectively (Figure 2b, d).

When the aging time was increased to 10 h, cubic nanoparticles were observed when the standard 2.45 GHz frequency was used (Figure 3a), but spherical morphologies were maintained when other microwave frequencies were used (Figure 3b–d). The average particle size of the nanoparticles was 77 ± 13 , 51 ± 13 , 59 ± 18 , and 54 ± 14 nm when 2.45, 3–5.5 (1 s), 4.0, and 5.5 GHz were used, respectively.

The particle size distribution of the products obtained at 10 h with various microwave frequencies was bimodal for all frequencies used, except for 4.0 and 5.5 GHz (Figure 6a). Prolonged processing time with the standard 2.45 GHz for 20 h resulted in well-faceted cubic nanoparticles with an average size of 98 ± 21 nm (Figure 4a). When aging was done in a conventional oven for 20 h, larger and irregular BaTiO₃ particles were obtained with an average size of 179 ± 75 nm (Figure 4b). Experiments performed using 5.5 and 4.0 GHz and a variable frequency of 3–5.5 GHz at varying sweep times of 5 and 1 s resulted in the formation of spherical particles with an average diameter of 54 ± 14 , 75 ± 18 , 70 ± 21 , and 55 ± 12 nm, respectively (Figure 4c–f). Low-magnification FESEM images of the sample prepared using 4 GHz and those prepared with a variable frequency (3–5.5 GHz) and with a longer bandwidth sweep time (5 s) show agglomerated clusters (insert, Figure 4e). As shown in Figure 6b, the particle size distribution was unimodal only for products prepared with 5.5 GHz, whereas conventional hydrothermal prepared samples showed a bimodal distribution with two peaks at 100 and 250 nm. Extension of

the processing time to 40 h did not have a significant influence on the particle size. The particle morphology with variable frequency remained spherical, whereas with 5.5 GHz usage, a mixture of spherical and cubiclelike particles was observed (Figure 5a–b). The average particle sizes of the conventional prepared barium titanate particles were larger than the microwave hydrothermal products (Figure 5c).

Transmission Electron Microscopy. TEM images of BaTiO₃, as well as selected area electron diffraction (SAED) and EDS analysis of the product obtained at 170 °C with variable frequency (3–5.5 GHz) and 1 s sweep time for 20 h, are presented in Figure 7. The bright-field TEM image shown in Figure 7a, b clearly shows well-dispersed spherical barium titanate nanoparticles. HRTEM data show that the particle diameter of these particles is around 50–60 nm, which is in agreement with that obtained from particle size analysis via FESEM. The electron diffraction from the sample shows a distinct ring pattern and can be completely indexed in the BaTiO₃ cubic *Pm3m* space group (Figure 8b, top insert). The lattice fringes were clearly observed from the HRTEM image, as shown in the bottom insert of Figure 7b. The distances between the neighboring lattice fringes are around 0.28 nm, which could be indexed to the *d* spacing of the (110) plane of either the tetragonal or cubic BaTiO₃ structure. The energy dispersive X-ray analysis (EDS) spectrum reveals the existence of barium, titanium, and oxygen.

Raman Spectroscopy. In general, X-ray diffraction gives an average and static symmetry, whereas the symmetry determined by Raman scattering is due to a change of the polarization of electrons caused by optical photons giving the local and dynamic symmetry. From the XRD patterns, the crystal structure of the prepared barium titanate was assigned with uncertainty to cubic barium titanate. Figure 8a, b shows the Raman scattering spectra from powders prepared at different conditions. The observed sets of Raman bands around 305, 517, and 716 cm⁻¹ for all samples prepared at 20–40 h can be assigned to tetragonal BaTiO₃, as reported in the literature.^{1,20} However, an additional Raman peak at 630 cm⁻¹ is observed for samples prepared using a variable frequency at 20 h with a 5 s sweep time and also when 4 GHz is used. This band is associated with hexagonal barium titanate.⁴ This peak at 630 cm⁻¹ was not observed in samples prepared with 2.45, 5.5, and 3–5.5 GHz variable frequency at 1 s sweep time or by conventional hydrothermal methods. With prolonged aging for 40 h, only Raman bands for the tetragonal phase were observed for samples prepared by conventional hydrothermal and with microwave hydrothermal methods at 3–5.5 GHz (1 s). However, bands associated with the high-temperature hexagonal phase coexisting with the tetragonal phase at room temperature are observed with particles processed using 5.5 GHz (Figure 8b).

The intensity of the 306 and 716 cm⁻¹ bands that are assigned to the tetragonal phase of BaTiO₃ was affected by the heating method, microwave frequency, and duration of the hydrothermal processing (Figure 8a, b).

Fourier Transform Infrared Spectroscopy. Figure 9 displays the representative IR spectra for the samples prepared under different microwave frequencies for 10–20 h. For all samples, the two broad characteristic bands at 570 and 420 cm⁻¹ are attributed to the Ti–O vibrational modes.^{1,21} The peaks around 1450–1640 cm⁻¹ are assigned to asymmetric and symmetric stretching modes of C=O and CO₃²⁻ respectively. Only samples prepared at 4 GHz for 10 h show a sharp absorption band around 3500 cm⁻¹, indicating possible OH⁻ incorporation into the BaTiO₃ lattices.¹

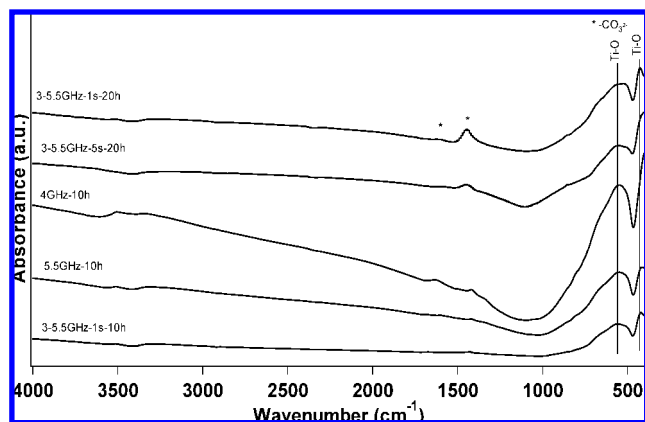


Figure 9. FT-IR spectra of BaTiO₃ samples prepared at different microwave frequencies.

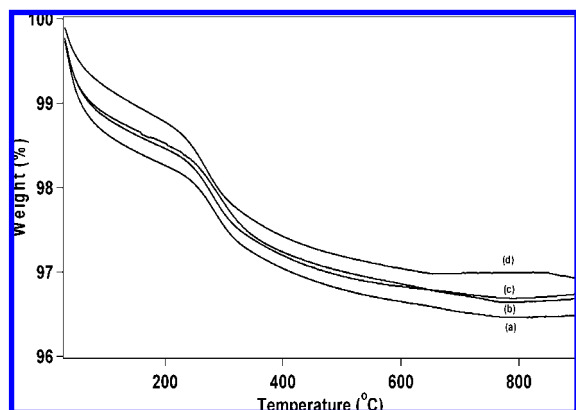


Figure 10. TGA of BaTiO₃ samples prepared at (a) 4 GHz, 10 h; (b) 3–5.5 GHz, 1 s, 10 h; (c) 5.5 GHz, 10 h; and (d) 3–5.5 GHz, 5 s, 20 h.

Thermal Analysis. TGA was performed to investigate the thermal behavior of barium titanate particles produced by microwave hydrothermal methods at different frequencies and aging times. Representative TGA curves are shown in Figure 10. Three major weight losses occur between 30 and 900 °C. For all samples, the first weight loss up to 240 °C is attributed to the desorption of physically adsorbed water. The second weight loss between 240 and 415 °C is ascribed to the loss of surface hydroxides.²² The third step (415–700 °C) is attributed to the loss of chemically bonded hydroxyl groups. The weight loss above 830 °C for the sample prepared under variable frequency with a 5 s sweep time for 20 h is due to the release of CO₂ from the decomposition of the BaCO₃ byproduct. This is consistent with IR and XRD data that showed the existence of BaCO₃ impurity in the sample.

Surface Area and Porosity. Table 2 presents the BET surface area, average pore diameter, and total pore volume of samples prepared under various microwave frequencies and aging times. The recorded isotherms for the samples prepared at various microwave frequencies are similar and correspond to the type II adsorption isotherms (IUPAC classification) with micropore filling at low P/P_0 and capillary condensation at high P/P_0 .²³ Samples prepared using 4.0 GHz fixed frequency and 3–5.5 GHz variable frequencies with a 5 s sweep time had no porosity. Raman studies of these samples showed the coexistence of the high temperature hexagonal phase with tetragonal BaTiO₃.

TABLE 2: BET Surface Areas, Average Pore Diameter, and Total Pore Volume of BaTiO₃ Prepared by MH at Various Microwave Frequencies

microwave frequency (GHz)	time (h)	BET surface area (m ² g ⁻¹)	av pore, ^b diam (Å)	total pore ^c vol (cm ³ /g)
2.45	10	12	—	—
4.00	10	37	233	0.215
5.50	10	36	255	0.228
3–5.5, sweep 1 s	10	19	275	0.128
4.00	20	1	—	—
5.50	20	26	—	—
3–5.5, sweep 1 s	20	24	301	0.180
3–5.5, sweep 5 s	20	1	—	—
5.50	40	7	—	—
3–5.5 sweep 1 s	40	31	—	—

^a —, property not determined. ^b By the BJH method. ^c Single point of total pore volume at $P/P_0 = 0.995$.

Discussion

Effect of Microwave Frequency on Phase Purity, Particle Size, Morphology, Surface Area, and Porosity of BaTiO₃ Nanoparticles. Effect on Phase. The XRD data showed that most of the samples obtained after 20 and 40 h have a polar and probably tetragonal structure because the (111) peak is appreciably narrower than that of the (200)/(002) peak. However, the formation of either cubic or tetragonal structures could not be excluded from the XRD data. This could be due to peak-broadening due to small particle sizes or the existence of cubic or pseudocubic structures. According to the Raman spectra, the crystal structure of most samples corresponds to the tetragonal phase due to the existence of phonon modes at 305 and 716 cm⁻¹ which are assigned to the tetragonal phase of BaTiO₃. The intensity of the 305 cm⁻¹ peak was found to be strongly dependent on the microwave frequency, duration of the hydrothermal treatment, and heating method. The observed broadening and weakening of this peak indicate loss of the tetragonal character, or the local symmetry is tetragonal but the slight tetragonal distortions seem to average out because of the disorder, resulting in a cubiclike ordering at longer distances, as suggested by Petkov et al.^{20b} We can assume that due to the size effect, the samples consist mainly of a global cubic structure with local tetragonal clusters, as suggested recently by Kolen'ko et al.,¹ Huang et al.,^{20c} and Shiratori et al.^{20d}

The phase purity of the obtained BaTiO₃ was influenced by the microwave frequency and bandwidth sweep times. For instance, at 4.0 GHz at the same temperature, size/quantity of precursor, and processing times (20 h), Raman analysis shows the presence of the impurity hexagonal BaTiO₃ phase. With variable frequency (3–5.5 GHz) using a 1 s sweep time; the impurity peak was not detected. Here, as expected, with VFMW experiments, the microwave radiation varies over a period of time, and the transient heating patterns vary constantly, not allowing the formation of hot spots.^{14,15} However, our results show that control of the sweeping time in the case of VFMW experiments is critical. Increasing the sweep time to 5 s results in a hexagonal phase impurity, which is an indication that even under variable frequency conditions, the transient heating patterns were not uniform, and hot spot formation was possible. In these samples, low magnification FESEM data showed extensive agglomerated clusters, a phenomenon that was not observed for the other samples.

Effect on Particle Size. The frequency and the bandwidth sweep times of microwave irradiation were found to influence the average particle size of the prepared barium titanate

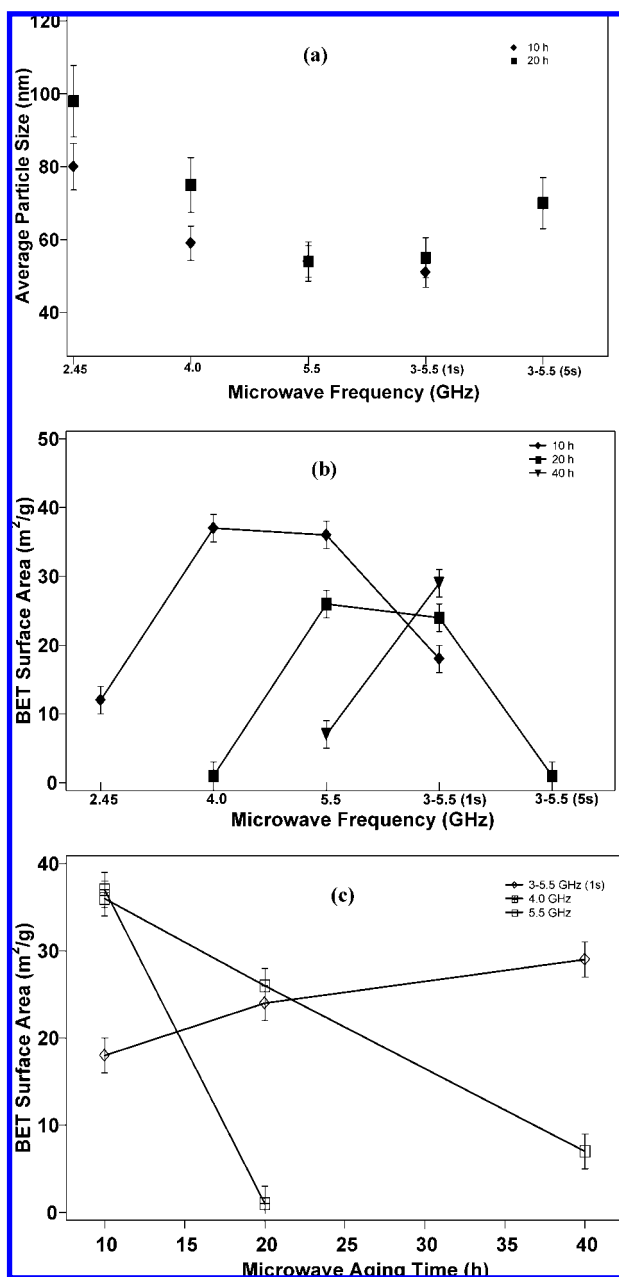


Figure 11. Relationship between (a) the average particle size of BaTiO₃ particles and microwave frequency at 170 °C, (b) BET surface area and microwave frequency, and (c) BET surface area and reaction time.

nanoparticles. The average particle size decreased with increasing microwave frequency, regardless of the aging time (Figure 11a). BaTiO₃ materials prepared at high microwave frequency (i.e., 5.5 GHz) and with variable frequency with 1 s bandwidth sweep times have smaller particle diameters. Increasing the variable frequency sweeping time from 1 to 5 s resulted in larger particle sizes. Particles prepared via conventional hydrothermal methods resulted in grains of larger, inhomogeneous sizes than those prepared with microwave hydrothermal methods under similar conditions. At low microwave frequency (2.45–4.0 GHz), the particle size increased with reaction time, whereas at high frequency (5.5 and 3–5.5 GHz, 1 s) the particle size essentially remained the same, even with increasing aging time. The growth process of BaTiO₃ at high frequency is clearly rather slow. Sun and co-workers recently reported that the particles grew faster with microwave heating than with conventional

heating.²⁴ Our finding that particle growth was slower with MH as compared to CH is due to the type of precursor and reaction temperature used. In their study,²⁴ barium hydroxide and a reaction temperature of ≥ 220 °C were used. In this study, barium chloride was used as the precursor at 170 °C. Previous reports support the formation of smaller BaTiO₃ particle sizes when barium chloride is used as a precursor instead of barium hydroxide.^{2,6,25}

Effect on Particle Morphology. The crystal shapes of the products prepared by microwave hydrothermal methods at lower microwave frequency (2.45 GHz) were generally cubic, whereas at other fixed frequencies, such as 4.0 or 5.5 GHz, and at variable frequency, they were spherical. We attribute this to differences in nucleation and crystal growth rates induced by the varying microwave frequency. The results suggest that at a lower microwave frequency, the nucleation process could be slower than crystal growth leading to cubic particles. When 2.45 GHz microwave irradiation was used, the particles became larger and more uniform with prolonged processing time. This could be attributed to Ostwald ripening as large particles grow at the expense of the dissolution of small ones.²⁴ However, at higher frequencies, the nucleation of the barium titanate nanoparticles could be faster than the crystal growth process and, consequently, result in spherical particles. Particle growth by a coarsening mechanism is much slower at high (5.5 GHz) and variable (3–5.5 GHz, 1 s) frequency. This is probably due to slower dissolution of the small particles at these frequencies (5.5 GHz and 3–5.5 GHz, 1 s), resulting in slower growth of the particles. Further investigation of the particle growth mechanism is ongoing.

Effect on Surface Area and Porosity. The results of surface area measurements of BaTiO₃ particles in Table 2 and Figure 11b show that the surface areas of the resultant materials were affected by the microwave irradiation frequency. The data also suggest a correlation between the surface area and the total pore volume of the particles. In these studies, the standard microwave frequency of 2.45 GHz was found to result in particles with different morphologies and particle size distributions. The surface area of these particles was generally lower than with 4.0–5.5 GHz and variable frequency usage with a 1 s sweep time. In general, with fixed frequency 4.0 and 5.5 GHz, the surface area decreased with aging time but increased with increasing aging time for variable frequency with a 1 s sweep time (Figure 11c). The measured mesoporosity is due to the agglomeration of the particles. Consistent with previous findings, the samples with hexagonal phase impurities were not porous, again a consequence of spatial distributions of microwave exposure. With variable frequency at low sweeping time (1 s), the microwaves penetrate the reaction mixture with different wavelengths, leading to rapid and more uniform heat distributions.¹³ In these reactions, hot spots that result in particle agglomeration and phase change could be eliminated.

Conclusion

In addition to reaction temperature and reactant compositions, the phases and sizes of BaTiO₃ synthesized by the microwave hydrothermal process can also be influenced by the microwave irradiation frequency and bandwidth sweep time. Syntheses of barium titanate with high (5.5 GHz) and variable (3–5.5 GHz, 1 s) frequency microwave irradiation were found to result in products with regular grain sizes and unimodal particle size distributions. However, products prepared via conventional heating under similar conditions exhibited bimodal particle size distributions with irregular grain sizes. Product prepared by the

standard fixed microwave frequency, 2.45 GHz, had microstructures different from those prepared at other frequencies. The surface areas of the particles prepared using variable frequency (3–5.5 GHz) with 1 s bandwidth sweep time increased with processing time. In contrast, the surface areas of nanomaterials prepared with fixed frequency decreased almost linearly with processing time.

Acknowledgment. We acknowledge support of the NSF-NIRT Award No. CTS-0304217. We thank Mr. James Romanow for providing access to the FESEM facilities in the Biology Department, University of Connecticut. We also thank Dr. Raymond Joesten for useful discussions and comments.

References and Notes

- (1) Kolen'ko, Y. V.; Kovnir, K. A.; Neira, I. S.; Taniguchi, T.; Ishigaki, T.; Watanabe, T.; Sakamoto, N.; Yoshimura, M. *J. Phys. Chem. C* **2007**, *111*, 7306.
- (2) Ma, Y.; Vilenko, E.; Suib, S. L.; Dutta, P. K. *Chem. Mater.* **1997**, *9*, 3023.
- (3) Cushing, B. L.; Kolesnichenko, V. L.; O'Connor, C. J. *Chem. Rev.* **2004**, *104*, 3893.
- (4) Yashima, M.; Hoshina, T.; Ishimura, D.; Kobayashi, S.; Nakamura, W.; Tsurumi, T.; Wada, S. *J. Appl. Phys.* **2005**, *98*, 014313.
- (5) O'Brien, S. O.; Brus, L.; Murray, C. B. *J. Am. Chem. Soc.* **2001**, *123*, 12085.
- (6) Dutta, P. K.; Asaiaei, R.; Akbar, S. A.; Zhu, W. *Chem. Mater.* **1994**, *6*, 1542.
- (7) Chen, H.-J.; Chen, Y.-W. *Ind. Eng. Chem. Res.* **2003**, *42*, 473.
- (8) Hakuta, Y.; Ura, H.; Hayashi, H.; Arai, K. *Ind. Eng. Chem. Res.* **2005**, *44*, 840.
- (9) Sun, W.; Li, J. *J. Am. Ceram. Soc.* **2006**, *89*, 118.
- (10) Sun, W.; Li, C.; Li, J.; Liu, W. *Mater. Chem. Phys.* **2006**, *97*, 481.
- (11) Tompsett, G. A.; Conner, W. C.; Yngvesson, K. S. *ChemPhysChem* **2006**, *7*, 296.
- (12) Galema, S. A. *Chem. Soc. Rev.* **1997**, *26*, 233.
- (13) Malinger, K.; Ding, Y. S.; Sithambaram, S.; Espinal, L.; Suib, S. L. *J. Catal.* **2006**, *239*, 290.
- (14) Conde, L. D.; Marun, C.; Suib, S. L.; Fathi, Z. *J. Catal.* **2001**, *204*, 324.
- (15) Conde, L. D.; Suib, S. L. *J. Phys. Chem. B* **2003**, *107*, 3663.
- (16) Caponetti, E.; Pedone, L.; Massa, R. *Mater. Res. Innovations* **2004**, *8*, 44.
- (17) Conner, W. C.; Tompsett, G.; Lee, K.-H.; Yngvesson, K. S. *J. Phys. Chem. B* **2004**, *108*, 13913.
- (18) Chen, X.; Wang, G.; Duan, Y.; Liu, S. *J. Phys. D: Appl. Phys.* **2007**, *40*, 1827.
- (19) Rasband, W. S. *ImageJ*; U.S. National Institutes of Health: Bethesda, MD, 1997–2007; <http://rsb.info.nih.gov/ij/>.
- (20) Venkateswaran, U. D.; Naik, V. M.; Naik, R. *Phys. Rev. B* **1998**, *58*, 14256. (b) Petkov, V.; Gateshki, M.; Niederberger, M.; Ren, Y. *Chem. Mater.* **2006**, *18*, 814. (c) Huang, T.-C.; Wang, M.-H.; Sheu, H.-S.; Hsieh, W.-F. *J. Phys.: Condens. Matter* **2007**, *19*, 476212. (d) Shiratori, Y.; Pithan, C.; Dornseiffer, J.; Waser, R. *J. Raman Spectrosc.* **2007**, *38*, 1300.
- (21) Busca, G.; Buscaglia, V.; Leoni, M.; Nanni, P. *Chem. Mater.* **1994**, *6*, 955.
- (22) Badheka, P.; Lee, B. I. *J. Eur. Ceram. Soc.* **2006**, *26*, 1393.
- (23) Leofanti, G.; Padovan, M.; Tozzola, G.; Venturelli, B. *Catal. Today* **1998**, *41*, 207.
- (24) Sun, W.; Pang, Y.; Li, J.; Ao, W. *Chem. Mater.* **2007**, *19*, 1772.
- (25) Jung, S. H.; Lee, J.-H.; Yoon, J. W.; Hwang, Y. K.; Hwang, J.-S.; Park, S.-E.; Chang, J.-S. *Mater. Lett.* **2004**, *58*, 3161.

JP7112818